The Journal of Immunology

# Reconciling Repertoire Shift with Affinity Maturation: The Role of Deleterious Mutations

Michele Shannon and Ramit Mehr

*J Immunol* 1999; 162:3950-3956; ;
http://www.jimmunol.org/content/162/7/3950



*The Journal of Immunology* is published twice each month by
The American Association of Immunologists, Inc.,
1451 Rockville Pike, Suite 650, Rockville, MD 20852

Print ISSN: 0022-1767 Online ISSN: 1550-6606.

# Reconciling Repertoire Shift with Affinity Maturation: The Role of Deleterious Mutations[1]

**Michele Shannon and Ramit Mehr[2]**

**The shift in Ab repertoire, from Abs dominating certain primary B cell responses to genetically unrelated Abs dominating subsequent "memory" responses, challenges the accepted paradigm of affinity maturation. We used mathematical modeling and computer simulations of the dynamics of B cell responses, hypermutation, selection, and memory cell formation to test hypotheses attempting to explain repertoire shift. We show that repertoire shift can be explained within the framework of the affinity maturation paradigm, only when we recognize the destructive nature of hypermutation: B cells with a high initial affinity for the Ag are less likely to improve through random mutations.** ***The Journal of Immunology,*** **1999, 162: 3950–3956.**

Repertoire shift is a phenomenon in which Abs dominating a primary response to Ag are severely depleted, or even absent, in the secondary response. The Abs that dominate the secondary response use variable (V) region genes that are different from those of the primary response. Repertoire shift is the rule rather than the exception in responses to T-dependent Ags, where hypermutation and affinity maturation occur, such as responses to the haptens (4-hydroxy-3-nitrophenyl)acetyl (1–7) and 2-phenyl-5-oxazolone (8–11), as well as in the response to influenza virus hemagglutinin (12, 13) and in rheumatoid factor responses (14). Repertoire shift is not to be confused with mutational drift of V region genes. Nor is repertoire shift merely a shift of the response from one epitope to another ("epitope shift;" Ref. 15), because it occurs in responses to single-epitope haptens and in response to individual viral protein epitopes (Ref. 16; M.S. and M. Weigert, unpublished data). Further, repertoire shift stands in apparent contradiction to the classical affinity-maturation paradigm, which predicts that dominant clones in the primary response would be most readily recruited into memory responses. The goal of the present study was to address the discrepancy between the affinity maturation paradigm and the observations on repertoire shift, using mathematical modeling and computer simulations of the dynamics of B cell clones to test our hypotheses.

Why would a B cell clone that is dominant in the primary response be missing from the secondary response? One possibility is that all the cells in this clone have undergone terminal differentiation into plasma cells. The choice of pathway—plasma or memory—may depend on the total sum of stimulating signals the cell receives (i.e., Ag receptor binding and cross-linking, second signals, and cytokines). For example, it can be envisioned that very strong stimulation, above some high threshold, $T_{high}$, can only lead to terminal differentiation into an Ab-producing plasma cell. Medium stimulation, below $T_{high}$ but above some lower threshold $T_{low}$, may lead to memory cell formation, although it does not necessarily exclude differentiation into plasma cells. Stimulation levels that fall below $T_{low}$ will not even activate a naive B cell, and hence will lead to no response at all. This hypothesis, which we call the "window" hypothesis, was initially inspired by studies of T cell selection in the thymus, where two different thresholds are assumed to exist for positive and negative selection (17). The window hypothesis is currently supported by the finding that memory cells (which have a higher affinity to the Ag than naive cells and hence may be assumed to experience a greater stimulation) more readily differentiate into plasma cells than naive cells (18). We show in this paper that the window hypothesis is sufficient to produce a repertoire shift similar to the one observed; however, it does not account for the effects of somatic hypermutation on memory cell formation.

When one considers the role of somatic hypermutation, a second way to reconcile repertoire shift with the affinity maturation paradigm becomes apparent: the primary Ab may fail to dominate the memory response because it is highly likely to suffer deleterious mutations. The process of affinity maturation is generally thought to improve the affinity of Abs to Ag through mutation and selection. If, however, a B cell clone begins with a relatively high affinity to the Ag, mutation would be more likely to decrease rather than increase its affinity. (We use here the term "affinity," even though the determining factor is probably the sum total of stimulation the cell receives due to the avidity of its receptor to the Ag and costimulatory signals. Hence, in the following text, "affinity" is used in this broad meaning, rather than in its exact biochemical definition.) At the same time, other, previously minor clones that can improve through mutation may become dominant clones. This hypothesis can best be visualized by assuming that, in the sequence space, the "landscape" of Ab affinity to the Ag is quite rugged, with many local "peaks" and "valleys" (19). The process of affinity maturation at most takes each Ab from where it started on this landscape only to the nearest local peak, which may not be the point with absolute highest affinity to the Ag in question. The Ab that dominated the primary response may thus end up in a local affinity peak that is lower than the final peaks reached by Abs that started in different, initially lower, points on the landscape (Fig. 1). As both sequences and affinities are experimentally measurable, it would be interesting to try to characterize the affinity landscape. Indication that this landscape is indeed rugged comes from findings of single mutations that confer a large (up to 10-fold) increase in affinity (2).

Department of Molecular Biology, Princeton University, Princeton, NJ 08544

Received for publication September 18, 1998. Accepted for publication January 8, 1999.

The costs of publication of this article were defrayed in part by the payment of page charges. This article must therefore be hereby marked *advertisement* in accordance with 18 U.S.C. Section 1734 solely to indicate this fact.

[1] This study was supported by National Institutes of Health Grant GM20964-25 for the study of genetics and regulation of autoimmunity.

[2] Address correspondence and reprint requests to Dr. Ramit Mehr, Department of Molecular Biology, Schultz Building, Washington Rd., Princeton University, Princeton, NJ 08544. E-mail address: ramit@princeton.edu



0022-1767/99/$02.00

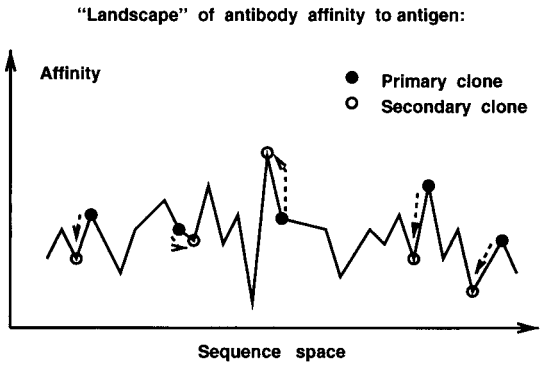


**FIGURE 1.** Illustration of our landscape hypothesis. The landscape lies on the sequence space, which is high-dimensional but is depicted here as one-dimensional for simplicity. B cell clones in the primary response (filled circles) have different values of affinity to the Ag. Mutation causes clones to drift along the landscape of affinity, in most cases leading to a decrease of a clone's affinity. Only in a few cases mutation would lead to an increase in affinity. As a result, among the clones appearing in the secondary response (open circles), the dominant clone would not necessarily be the one that dominated the primary response.

## Modeling Differentiation and Competition of B Cell Clones

As only the end results of mutation and clonal selection can be observed experimentally, we chose to use mathematical modeling and computer simulations of the dynamics of B cell clones to test the above hypotheses. Our model consists of an array of B cell clones that can proliferate, differentiate, and mutate in response to antigenic stimulation (Fig. 2). Each clone $i$ is assigned a number $\sigma_i$ which represents the sum of the many stimulating signals a cell in this clone is receiving, including the interaction between the Ag receptor of the cell and the Ag. Below we sometimes refer to $\sigma_i$ as "affinity," because affinity to the Ag is the most important factor in the stimulation of the B cell. Members of each clone may be either

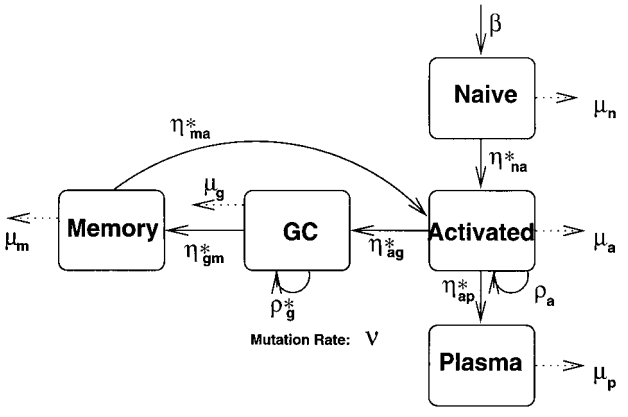


**FIGURE 2.** B cell model. The diagram represents B cell subsets: naive, activated, GC, memory, and plasma B cells in a single clone. Differentiation and proliferation pathways (solid arrows) and death (dotted arrows) are shown. Processes depending on Ag concentration are marked by an asterisk (∗). There is a constant input into the naive cell compartment from the bone marrow with a rate $\beta$. In the presence of Ag naive cells are activated in an affinity-dependent manner at a rate $\eta_{na}$. Activated cells may either differentiate into plasma cells (at a rate $\eta_{ap}$) or GC cells (at a rate $\eta_{ag}$). GC cells become memory cells at a rate $\eta_{gm}$, and memory cells may be reactivated at a rate $\eta_{ma}$. Proliferation rates for activated and GC cells are $\rho_a$ and $\rho_g$, respectively. The equations governing these processes are given in *Appendix 1*.

naive (with the number of naive cells represented by $N_i$), activated ($A_i$), germinal center ($G_i$), memory ($M_i$), or plasma ($P_i$) cells. Thus, the temporal evolution of cell numbers in each subset within each clone are described by a differential equation of the form

$$change/time = input + proliferation - diferentiation - death.$$

For each compartment, "input" refers to incoming cells from the previous compartment; in the equation for naive cells this is replaced by a term representing constant input from the bone marrow. Proliferation is Ag-dependent, and assumed to occur only in the activated and germinal center (GC)[3] compartment. "Differentiation" refers to the emigration of cells to the next compartment, and it is also Ag dependent, and proportional to the affinity of the cell's receptor to the Ag. Cell death may occur in all compartments. The equations are given explicitly in *Appendix 1*.

The transition from GC to memory cells is assumed to be Ag-independent, and memory cells can also be re-activated by Ag. In the model, Ag depletion results from consumption by activated and plasma cells. Sequestration on follicular dendritic cells keeps Ag in the GCs much longer than it remains outside the GCs (20). Hence, we assume that Ag remains available for cells in the GCs much longer than for activated cells outside the GCs (equations for Ag decay are given in *Appendix 1*).

Parameters for the simulations were taken from the literature whenever possible. Production/division rates and lifespans of lymphocytes in peripheral compartments were obtained from studies utilizing various labeling techniques (reviewed in Refs. 21–24), which also give steady-state B cell numbers (25). From these data, death rates and rates of transitions between compartments can be obtained using mathematical modeling of B cell populations (26, 27). We have assumed that only activated and GC B cells divide. In our model, the differences between naive and memory B cells are only a matter of rates: memory B cells have a much lower death rate and a much higher activation rate than naive cells (18). The numerical values of parameters used in our simulations are given in *Appendix 2*.

## Results

For a single clone, a mathematical analysis of the model's equations may have been sufficient. However, we are interested in the much more complex dynamics of affinity maturation that emerge when a large number of clones compete for a single Ag. Hence we turn to computer simulations of our model.

### *The affinity maturation paradigm does not generate repertoire shift*

First, we performed simulations of the model that did not include mutations nor any other attempt to generate repertoire shift. It is possible to model affinity maturation without mutations, as long as we refer to affinity maturation as occurring on the level of cell populations, and not individual cells. These simulations generated the picture predicted by the affinity maturation paradigm: clones that dominated the primary response continued to dominate the secondary response, and the average affinity increased.

The different clones were assigned their $\sigma_i$ numbers using the arbitrary formula $\sigma_i = 1/i^2$. Thus, $\sigma_1 = 1$, $\sigma_2 = 0.25$, $\sigma_3 = 0.11$, and so on. This was chosen with the sole purpose of distinguishing between clones on the basis of the strength of the stimulation they receive from the Ag and other costimulatory signals. We simulated 10 clones, with clone 1 having the highest affinity and clone 10 the lowest affinity.

[3] Abbreviations used in this paper: GC, germinal center; CDR, complementarity-determining region.

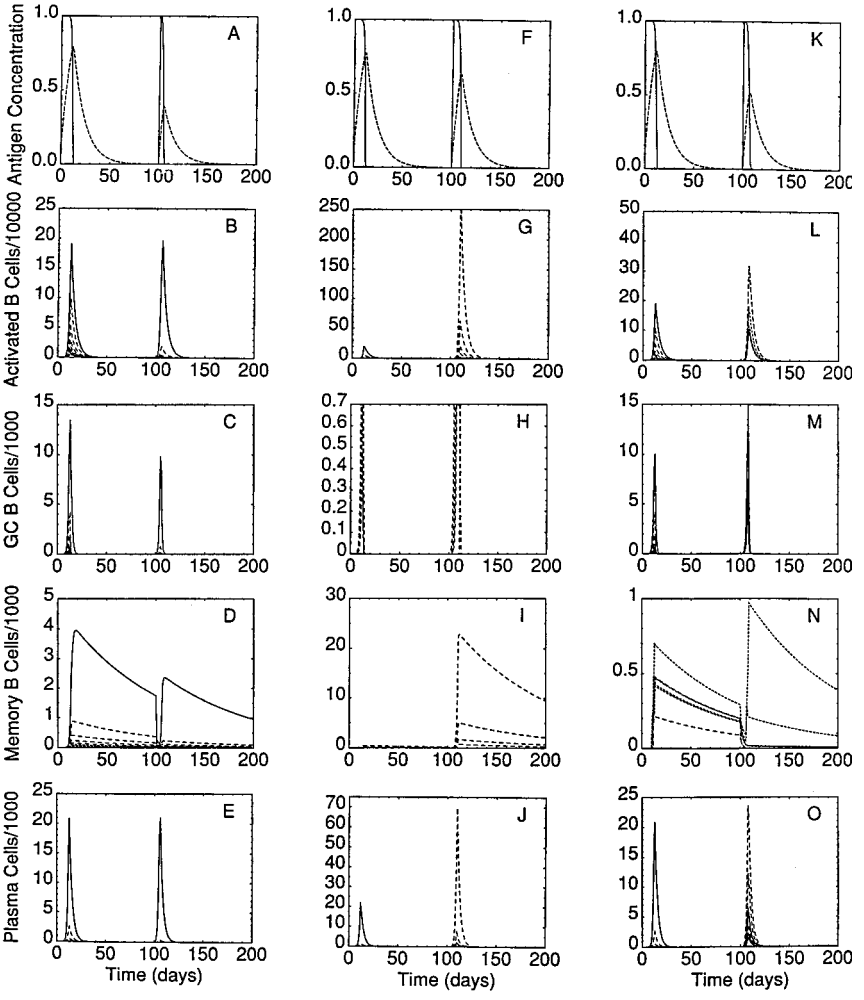


**FIGURE 3.** Simulations of B cell dynamics in three different scenarios. *A–E*, A simulation of the prediction of the affinity maturation paradigm. *F–J*, A simulation of the window hypothesis. *K–O*, A simulation with mutations, based on the landscape hypothesis. In all simulations, Ag was injected at times 0 and 100 days. The following quantities were plotted. *A*, *F*, and *K*, Ag concentration outside ($R$, solid line) and inside ($R_G$, dashed line) of the GCs. *B*, *G*, and *L*, Activated B cells ($\times 10^4$), plotted by clone: clone 1 is plotted as a solid line, clones 2–5 as dashed lines, and clones 6–10 as dotted lines. Note that activated cell numbers in the secondary response are an order of magnitude higher in the simulation of the window hypothesis (*G*) than in the other two simulations, as discussed in the text. *C*, *H*, and *M*, GC cells ($\times 10^3$), also plotted by clones. The scale in plot *H* was enlarged to show detail: the solid line representing the highest-affinity clone (clone 1) appears only in the primary response, but not in the secondary response. *D*, *I*, *N*, Memory B cell clones ($\times 10^3$). *E*, *J*, and *O*, Plasma B cell clones ($\times 10^3$). Parameters for these simulations are given in *Appendix 2*. The different clones were assigned their $\sigma_i$ numbers using the arbitrary formula $\sigma_i = 1/i^2$. Thus, $\sigma_1 = 1$, $\sigma_2 = 0.25$, $\sigma_3 = 0.11$, and so on. Additional parameter values in simulation *K–O* were: $\alpha = 4$, $T_s = 5$, and the mutation rate: $\upsilon = 1$ (see *Appendix 3* for details).

A representative simulation is shown in Fig. 3, *A–E*. In this simulation, the Ag is eliminated much more rapidly in the secondary response than in the primary response (Fig. 3*A*). The B cell clone that dominated the primary response (clone 1, which has the highest $\sigma$, plotted using solid lines) continues to dominate the secondary response. This is true for all relevant cell subsets: activated (Fig. 3*B*), GC (Fig. 3*C*), memory (Fig. 3*D*), and plasma cells (Fig. 3*E*). The lower affinity clones (clones 2–5 were plotted using dashed lines, and clones 6–10 as dotted lines) reach lower peak numbers, in descending order according to their $\sigma$ values in all subsets.

In this simulation, the average affinity does increase (i.e., affinity maturation does occur on the cell population level) because the fraction of highest-affinity cells dramatically increases from the primary to the secondary response (Fig. 3, *B–E*). The total numbers of cells at the peak of each response, the timing of the peak, and the decline of the response all agree with experimental observations (20, 28), confirming that we have chosen a reasonable set of parameter values. However, in these simulations there is no repertoire shift.

### *The window hypothesis*

In a second set of simulations, we included in our simulations a window hypothesis, stating that very high affinity (that is, $\sigma_i$ above some high threshold, $T_{high}$) can only lead to terminal differentiation into an Ab-producing plasma cell. Cells with affinity below a lower threshold, $T_{low}$, never get activated. We have chosen $T_{low} = 0.03$, such that, with the above-chosen values of $\sigma_i$, only clones 1–5 can become activated. We have also chosen $T_{high} = 0.3$, meaning that all cells belonging to clone 1 (the clone with the highest affinity) are driven to differentiation to plasma cells.

Not surprisingly, these simulations exhibit repertoire shift, because our choice of the thresholds prohibits the primary dominant clone from forming memory cells (Fig. 3, *F–J*; in *H*, the scale is adjusted to show that the solid line representing clone 1 is missing from the secondary response). The small numbers of plasma cells of clone 1 that do appear in the secondary response are due to activation of naive cells, which is much slower than that of memory cells (Fig. 3*J*). However, the picture is not completely realistic: Ag clearance is not much faster in the secondary response, because only low-affinity clones (which clear Ag more slowly) participate in this response (Fig. 3*F*). As a result, cell numbers in the secondary response are much higher than those of the primary response, because they are allowed more time to proliferate (Fig. 3*G*).

### *The effect of mutations*

Even if the picture obtained using the window hypothesis had been completely realistic, it is not known whether such defined differentiation thresholds exist. Hence the question arises whether repertoire shift can be generated directly by simulating the processes of somatic hypermutation and Ag-driven selection.

In the simulations described below, mutations were modeled by taking cells from the GC compartment and allowing them to "mutate," with a rate $\upsilon$, and obtain new values of $\sigma_i$. Values given in

the literature for hypermutation rate are as high as $2.5 \times 10^{-3}$/bp/division (12, 13). Since each cell harbors about 1000–2000 bp of mutable V genes, this rate generates roughly 1 mutation/cell/division. This was the value we used in most simulations.

The next point to consider is how many of the mutations are actually relevant to clonal selection. One-quarter of all mutations can be expected to be silent, and therefore irrelevant, due to the properties of the genetic code. Independently, the complementarity-determining regions (CDRs) account for roughly one-quarter of the length of the V genes. Hence, assuming mutations are random, one-quarter of V gene mutations are expected to occur in the CDRs, the rest occurring in the framework regions. Shlomchik et al. (29) found that about half of all framework mutations are lethal, and the other half are neutral. Replacement mutations in the CDRs, however, may be lethal, neutral, or even advantageous depending on how they change the Ab binding site, and the probabilities for this are Ag-dependent. In our simulations, we have set these probabilities such that most mutation-induced affinity changes are small, while large "leaps" in affinity are relatively rare. (The details of our stochastic model of the mutational process are given in *Appendix 3*.) This incorporates our landscape hypothesis in the model.

Selection is applied in our model in the following way. If the postmutation affinity, $\sigma_{new}$, is smaller that the premutation affinity, $\sigma_{old}$, then the cell fails selection and dies. A cell is positively selected, forming a new subclone, only if $\sigma_{new} > T_s\sigma_{old}$, with $T_s$ representing a threshold parameter. If $\sigma_{old} < \sigma_{new} < T_s\sigma_{old}$, meaning there is only moderate improvement, this improvement is ignored. This enables us to save the computation of clones that would be out-competed and never contribute significantly to any response, as we found in preliminary simulations (data not shown).

The model assumes that new clones being formed in each GC compete only among themselves, and not with clones in other GCs. This is why $\sigma_{new}$ is only compared to $\sigma_{old}$. There is no reason to assume otherwise, because GCs are spatially distinct structures (3).

Simulations with mutation and selection thus implemented give a realistic picture of repertoire shift (Fig. 3, *K–O*). This picture is much richer than that observed with the arbitrary window hypothesis. Here, not only one but the four highest-affinity primary clones never succeed in generating higher-affinity mutants, and hence do not produce memory cells, in spite of these four clones' domination of the primary response among activated GC and plasma cells. Note especially the activated cells (Fig. 3*L*): the primary response is dominated by (in descending order of peak cell numbers) clones 1, 2, 3, and 4, which are the four highest initial affinity clones; while the secondary response shows clones 5, 6, 7, and 8 (which initially had intermediate affinities) as the dominant ones. This picture is repeated in the GCs (Fig. 3*M*) and in the plasma cell populations (Fig. 3*O*). Selection is carried even further in the memory pool: the order of clones selected into the memory pool after the primary response is 6, 5, 7, 8, 9, and 4 (Fig. 3*N*), but after the secondary response, selection results in dominance of two clones only (clones 6 and 7), which initially had intermediate affinities. The mutational process is more destructive than productive for the four highest-initial-affinity clones. The secondary response is dominated by the next five clones (in order of decreasing initial affinity to the Ag), because these are the clones that have managed to produce improved affinity mutants and hence generate memory cells.

It is worth noting that if we extend our simulations to include a third and even a fourth antigenic challenge, the clones that dominate the secondary response continue to dominate subsequent responses (data not shown). Additional challenges only serve to further increase the size of the memory cell pool. This behavior is in agreement with experimental observations. In our opinion, this result confirms our assumption that there are basic differences between naive and memory B cells: the much more rapid activation and expansion of memory cells lead to elimination of the Ag before somatic hypermutation could exert significant deleterious effects on this population (18). Furthermore, Abs with maximal affinities to the Ag are likely to have been formed already by the secondary response, so that the probability of these Abs being outcompeted by newer, even better Abs, becomes very small. The net result is that repertoire shift only occurs between the primary and secondary responses, while subsequent challenges do not lead to further shifts.

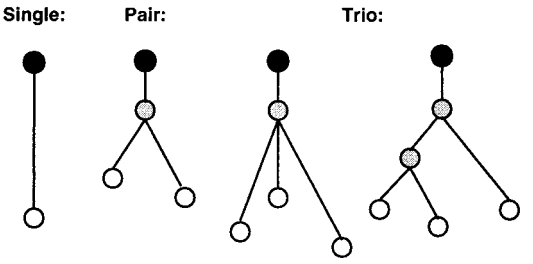


**FIGURE 4.** Types of lineage trees observed experimentally. Each circle represents a clone; filled circles represent germline clones. Intermediate clones (gray circles) were not always observed, but could be deduced from the sequences. The length of each branch represents the number of mutations. Trees with a single branch were most common; trees with two branches were less common, and trees with three branches were rare (see text).

Recent findings (7) suggest that hypermutation and Ag-driven selection go on, albeit at a much slower rate, for several months after the GC response has dwindled. This may ensure that the maximal-affinity Abs will be already generated by the end of the primary response, and will become dominant upon a secondary challenge.

A study of the dependence of these results on parameter values has shown the following. First, repertoire shift is more pronounced if the distribution of mutations is made narrower; that is, if advantageous mutations are more rare. This finding supports our key point, that repertoire shift results from the destructive aspect of hypermutation on Abs that had a high affinity to the Ag prior to mutation. Second, as expected, a similar effect is observed when increasing $\alpha$, the parameter that determines the relative advantage conferred by mutations, or $T_s$, the stringency of the selection operating on newly generated mutants (results not shown).

## Lineage Relationships Reflect Multiple Rounds of Mutations

As an additional test for our model, we have studied the lineage relationships between mutants generated in our simulations, and compared them to lineage "trees" deduced from the sequences of B cell hybridomas generated in the response to influenza virus (M.S., et al. unpublished data). The experimentally generated lineage trees reflect multiple rounds of mutations for each germline V gene that participated in the primary response. These trees are not highly branched, and each branch was long, meaning that many mutations occurred. We believe the "pruned" shape of these trees is evidence for the destructive character of somatic hypermutation (Fig. 4). This finding is supported by evidence showing that trees generated from clones during the peak of the primary response are much more "bushy" (4), and that the trees become less bushy as the response progresses (5).

In our simulations, only a narrow range of parameters, specifically a high rate of mutation ($\upsilon = 1$) combined with a low probability of advantageous mutations ($\alpha = 4$, SD of the distribution of $r_s$ is 0.1), and a stringent competition between newly formed B cell clones ($T_s = 5$), gives rise to tree shapes similar to those observed. (For example, in the simulation given in Fig. 3, *K–O*, most clones had at most two "branches," and clones with three or more branches were rare.) This further supports our key point.

It is not as yet clear whether the distribution of "tree shapes" deduced from the experiment reflects the actual distribution in the animal during the secondary response, or is caused by a sampling effect, since the experiments did not detect all mutants generated in each animal. Our simulations enable us to test the effects of various ways of sampling the mutant clones. Three different methods of sampling—random sampling, sampling the clones with highest affinity to Ag, or those with highest cell numbers at day 3 of the secondary response (when experimental clones are obtained)—always resulted in a distribution of clones resembling the original distribution (data not shown). Thus we believe that the experimentally observed tree shape distribution probably reflects the distribution within the animal, and is not an artifact of a small sample size.

## Discussion

In spite of the prevalence of repertoire shift in many well-studied responses, to the best of our knowledge there has been no attempt to reconcile the discrepancy between repertoire shift and the affinity maturation paradigm. Berek and Milstein (8) suggested that repertoire shift is the result of cell population dynamics, but this point was not developed further. Oprea and Perelson (30) suggested that the higher the affinity of an Ab to the Ag, the less likely it is to improve, but the latter study did not address repertoire shift.

We have utilized two approaches to study how memory responses are generated. We began with the heuristic window hypothesis which states that memory cells will only be formed out of those B cell clones that experienced low-level stimulation by Ag during the primary response, while clones experiencing higher level stimulation will all be driven toward terminal differentiation and subsequent extinction. The results have clearly shown a shift in the B cell repertoire, provided that memory cells are unlikely to be formed by B cell clones which have a high affinity to the Ag during the primary response.

We then simulated the landscape hypothesis which postulates that, once somatic hypermutation and affinity maturation begin operating on all responding clones, memory cells from low-affinity clones may mutate into B cells whose receptors have higher affinity to the Ag than that of the clone that dominated the primary response. Mutations in the best primary clone, on the other hand, are more likely to lead to reduction in affinity, so that this clone will be out-competed in the race to form memory B cells. This hypothesis, which is based on the dynamics of somatic hypermutation, appears to capture the causes of repertoire shift in more detail. Within this model, repertoire shift is more pronounced the more unlikely we assume advantageous mutations are. This result elucidates the destructive effect of hypermutation on the primary B cell repertoire. Our assumptions are further supported by the shape of B cell lineage trees deduced from observed clones.

Note that we have not included in the model any artificial "turning on" of processes such as GC seeding or mutation, features that appear in all previous models of the B cell response (26, 27, 29–32). Our model captures the experimentally observed dynamics, including the mutational processes, only by virtue of appropriate choices of transition rates. Nor have we assumed any saturation limits for cell proliferation in the various compartments. Cell populations rise only as a result of antigenic stimulation at the beginning of each response, and then fall as Ag is being eliminated by B cells and Abs.

Foote and Milstein (11) suggested that, while the determination of the Ab dominating the primary response is done on the basis of affinity, the selection of memory B cells is determined by the on-rate. That is, B cells would "win the race" to become memory cells if they bind Ag more rapidly, thus out-competing slower-binding cells from binding to the few antigenic sites available in the GCs. The results of our theoretical study above show that this interpretation may be acceptable, provided we assume that mutations that improve the on-rate of binding are relatively rare. More experimental measurements of the affinities and on-rates of receptor-Ag interactions, in both the primary and the secondary responses, are required in order to examine this interesting possibility.

Current findings (7, 33) suggest that not all plasma cells die in the spleen 3–4 days after their formation, as previously assumed. A small subset of plasma cells in the bone marrow, which consists of about 3% of the plasma cells produced in a given response, is long-lived and is responsible for maintaining the serum levels of Abs for months after the full B cell response dies out. We have added this feature into the model, checking whether this would give a faster elimination of Ag in the secondary response than that achieved in the previous simulations. A slightly faster elimination of Ag has indeed been achieved (data not shown), but only if these long-lived plasma cells were not too long-lived (death rate was 0.03/day, 10-fold lower than that of "normal" plasma cells). If the death rate was made one more order of magnitude lower (0.003/day), there were so many plasma cells left that there was no need for memory cells, and no repertoire shift has occurred. As noted previously (33), if plasma cells generated in the primary response were long-lived, then isotype switching and affinity maturation were less likely to occur. Long-lived bone marrow plasma cells appear to be postselection cells; that is, cells that have been formed after affinity maturation has taken place. Our results support this scenario.

A related question is whether the average affinity of Abs to the Ag increases between the primary and the secondary response (7). (Here we use the word "affinity" in its commonly used meaning.) Not all studies which have attempted to measure the change in average affinity, e.g. studies on the response to vesicular stomatitis virus (16), have detected a significant change in Ab avidity to the Ag. The latter study concluded that the main effect of somatic hypermutation on the primary Abs must be destructive, making way for the appearance of new clones, which supports our present conclusion.

The present study is the first attempt to rigorously test a hypothesis aimed at explaining repertoire shift. Our computer simulations show that the destructive force that somatic hypermutation exerts on the dominating clones, in and of itself, is sufficient to explain repertoire shift. Studies of the humoral immune response have traditionally focused on the positive aspect of somatic hypermutation. The paradigm of affinity maturation, stating that B cells taking part in the secondary response are "improved versions" of those that dominated the primary response, is often confused with somatic hypermutation. One should keep in mind that somatic hypermutation is only the mechanism generating candidates for affinity improvement, on which selection then operates. One must remember that affinity-improving mutation is more likely to be a rare event in a multitude of deleterious mutations. A thorough understanding of the immune response must acknowledge the destructive aspect of hypermutation.

## Appendix 1. The Differential Equations of Our Model

The temporal evolution of cells in each clone can be summarized by the following equations,

$$\frac{dN_i}{dt} = \beta + (\rho_n - \mu_n - \mathrm{R}\sigma_i\eta_{na})N_i \quad (1)$$

$$\frac{dA_i}{dt} = R\sigma_i\eta_{na}N_i + \mathrm{R}\sigma_i\eta_{ma}M_i + [R\rho_a - \mu_a - R\sigma_i(\eta_{ag} + \eta_{ap})]A_i \quad (2)$$

$$\frac{dG_i}{dt} = R\sigma_i\eta_{ag}A_i + (\rho_g\sigma_i R_G - \mu_g - \eta_{gm})G_i \quad (3)$$

$$\frac{dM_i}{dt} = \eta_{gm}G_i + (\rho_m - \mu_m - R\sigma_i\eta_{ma})M_i \quad (4)$$

$$\frac{dP_i}{dt} = R\sigma_i\eta_{ap}A_i + (\rho_p - \mu_p)P_i \quad (5)$$

where $\rho_j$ denotes the daily proliferation rate of subset $j$, $j$ representing $n$ (naive), $a$ (activated), $g$ (GC), $m$ (memory), or $p$ (plasma). Similarly, $\eta_{jk}$ is the daily rate of transition from subset $j$ to subset $k$, and $\mu_j$ is the daily cell death rate of subset $j$.

Thus, naive B cells are being "born" out of the bone marrow with a rate of $\beta$ cells per clone per day, die with a rate $\mu_n$, or become activated with a rate $\eta_{na}$. Once activated, B cells proliferate with a rate $\rho_a$, die with a rate $\mu_a$, become plasma cells with a rate $\eta_{ap}$, or go to the GCs with a similar rate $\eta_{ag}$. Similar equations hold for activated, GC, memory, and plasma cells.

Note that our model is based on the assumption that memory and plasma cells belong to the same lineage. This assumption seems to be most strongly supported by experimental data (4, 34), and our model shows that this assumption explains the data well.

$R$ denotes the relative antigen concentration outside of the GCs (measured relative to its initial concentration, so that the maximum concentration equals 1), and it decreases with time according to:

$$\frac{dR}{dt} = -R\frac{\sum_{i=1}^{K}(A_i + fP_i)\sigma_i}{B_{max}} \quad (6)$$

where $f$ is the factor denoting the relative efficiency of plasma cells, compared to activated cells, in eliminating the Ag ($f \gg 1$), and $B_{max}$ is a scaling factor. $R_G$, the Ag concentration inside the GCs, which is assumed to decrease much more slowly than that of free Ag due to sequestration on follicular dendritic cells, varies with time according to:

$$\frac{dR_G}{dt} = \gamma R - \delta R_G \quad (7)$$

that is, Ag from outside the GCs flows inside with a rate $\gamma\ \mathrm{day}^{-1}$, and is lost with a rate $\delta\ \mathrm{day}^{-1}$. Most transitions (naive to activated, activated to GC or to plasma, memory to activated), and the proliferation of activated or GC cells, depend on Ag concentration in a linear manner. Ag-dependent transitions are multiplied by $\sigma_i$ to distinguish between clones with different strengths of interaction with the Ag. The transition from GC to memory cells is Ag-independent. Memory cells can also be re-activated by Ag. Mutations occur only in the GC compartment and are expressed as changes in the value of $\sigma_i$, as explained in *Appendix 3*.

## Appendix 2. Model Parameters

The rates of cell birth, proliferation, death and differentiation, used in our simulations, are given in Tables I and II. In addition, we used: time step = 1 day; length of the simulation: up to 200 days; and $B_{max} = 10^6$. The plasma cell factor $f$ was varied between 1 and $10^4$.

## Appendix 3. Modeling Mutations

Table I. *Parameters for (murine) B cell simulation: values found in the literature (references are in parentheses)*

| B Cells | Entry | Division | Death |
|---|---|---|---|
| Naive | 10–20/clone; $10^6$ clones/day | 0 | Lifetime 2 days (0.5/day) |
| Activated | | 1 div/8–16 h 1.5/day (19) | 0.1–1.0/day (18) 0.2/day (19) |
| GC | | Every 6–7 h | |
| Memory | | Half-life to div or death 6 weeks (16) | Half-life to div or death 6 weeks (16) |
| Plasma | | 0 | Lifetime 4 days 0.3/day (19) |

Table II. *Parameters for (murine) B cell simulation: values used in our simulations*

| B Cells | Entry Rate ($\mathrm{day}^{-1}$) | Proliferation Rate ($\mathrm{day}^{-1}$) | Death Rate ($\mathrm{day}^{-1}$) |
|---|---|---|---|
| Naive ($N_i$) | $\beta = 20$ cells | $\rho_n = 0$ | $\mu_n = 0.5$ |
| Activated ($A_i$) | $\eta_{na} = 0.001$ $\eta_{ma} = 1.0$ | $\rho_a = 1.5$ | $\mu_a = 0.2$ |
| GC ($G_i$) | $\eta_{ag} = 0.2$ | $\rho_g = 0.2$ | $\mu_g = 0.1$ |
| Memory ($M_i$) | $\eta_{gm} = 1.0$ | $\rho_m = 0$ | $\mu_m = 0.01$ |
| Plasma ($P_i$) | $\eta_{ap} = 0.1$ | $\rho_p = 0$ | $\mu_p = 0.3$ |

Based on the available data discussed in the text, we have used the following considerations. The probability that a mutation is lethal due to a replacement in the framework region is $p_{lethal} = \frac{3}{4} \times \frac{3}{4} \times \frac{1}{2} = 0.28125$. The probability that a mutation will be a silent mutation anywhere, or a neutral replacement mutation in the framework region, is $p_{sn} = \frac{1}{4} + \frac{3}{4} \times \frac{3}{4} \times \frac{1}{2} = 0.53125$. Hence, once a cell mutates, it will die with a probability $p_{lethal}$, or do nothing with a probability $p_{sn}$. The remaining $(1 - p_{lethal} - p_{sn})$ of all mutations are considered mutations in the CDRs and dealt with as follows. The affinity $\sigma_{new}$ of the mutant receptor is determined as a random multiple of the old value $\sigma_{old}$, according to the following formula:

$$\sigma_{new} = \sigma_{old}10^{\alpha(r_s - \sigma_i)}, \quad (8)$$

where $\alpha$ is an exponent giving the maximum log improvement in the affinity (e.g., $\alpha = 3$ means that the affinity can improve at most 1000-fold in one round of mutation). $r_s$ is a random number providing stochasticity. To include our landscape hypothesis—that the better the receptor is to begin with, the less likely it is to improve through mutation—we take the random number $r_s$ from the positive half of a Gaussian distribution with a small SD (typically 0.1). Thus, higher values of $r_s$, and large "leaps" in affinity (cases in which $r_s \gg \sigma_i$), are very unlikely. The smaller the standard deviation of the distribution of $r_s$, the more rare these leaps.

## Acknowledgments

Useful discussions with Drs. Martin Weigert, Philip Seiden, and Samuel Litwin are gratefully acknowledged.

## References


1. Reth, M., G. J. Hammerling, and K. Rajewsky. 1978. Analysis of the repertoire of anti-NP antibodies in C57BL/6 mice by cell fusion. I. Characterization of antibody families in the primary and hyperimmune response. *Eur. J. Immunol. 8:393.*
2. Allen, D., T. Simon, F. Sablitzky, K. Rajewsky, and A. Cumano. 1988. Antibody engineering for the analysis of affinity maturation of an anti-hapten response. *EMBO J. 7:1995.*
3. Jacob, J., R. Kassir, and G. Kelsoe. 1991. In situ studies of the primary immune response to (4-hydroxy-3-nitrophenyl)acetyl. I. The architecture and dynamics of responding cell populations. *J. Exp. Med. 173:1165.*
4. Jacob, J., and G. Kelsoe. 1992. In situ studies of the primary immune response to (4-hydroxy-3-nitrophenyl)acetyl. II. A common clonal origin for periarteriolar lymphoid sheath-associated foci and germinal centers. *J. Exp. Med. 176:679.*
5. Jacob, J., J. Przylepa, C. Miller, and G. Kelsoe. 1993. In situ studies of the primary immune response to (4-hydroxy-3-nitrophenyl)acetyl. III. The kinetics of V region mutation and selection in germinal center B cells. *J. Exp. Med. 178:1293.*
6. Han, S., B. Zheng-B, J. Dal-Porto, and G. Kelsoe. 1995. In situ studies of the primary immune response to (4-hydroxy-3-nitrophenyl)acetyl. IV. Affinity-dependent, antigen-driven B cell apoptosis in germinal centers as a mechanism for maintaining self-tolerance. *J. Exp. Med. 182:1635.*
7. Takahashi, Y., P. R. Dutta, D. M. Cerasoli, and G. Kelsoe. 1998. In situ studies of the primary immune response to (4-hydroxy-3-nitrophenyl)acetyl. V. Affinity maturation develops in two stages of clonal selection. *J. Exp. Med. 187:885.*
8. Berek, C., and C. Milstein. 1987. Mutation drift and repertoire shift in the maturation of the immune response. *Immunol. Rev. 96:23.*
9. Griffiths, G. M., C. Berek, M. Kaartinen, and C. Milstein. 1984. Somatic mutation and the maturation of immune response to 2-phenyl oxazolone. *Nature 312:271.*
10. Berek, C., G. M. Griffiths, and C. Milstein. 1985. Molecular events during maturation of the immune response to oxazolone. *Nature 316:412.*
11. Foote, J., and C. Milstein. 1991. Kinetic maturation of an immune response. *Nature 352:530.*
12. Clarke, S. H., L. M. Staudt, J. Kavaler, D. Schwartz, W. U. Gerhard, and M. G. Weigert. 1990. V region gene usage and somatic mutation in the primary and secondary responses to influenza virus hemagglutinin. *J. Immunol. 144:2795.*
13. Kavaler, J., A. J. Caton, L. M. Staudt, and W. U. Gerhard. 1991. A B cell population that dominates the primary response to influenza virus hemagglutinin does not participate in the memory response. *Eur. J. Immunol. 21:2687.*
14. Randen, I., V. Pascual, K. Victor, K. M. Thompson, Ø. Førre, J. D. Capra, and J. B. Natvig. 1993. Synovial IgG rheumatoid factors show evidence of an antigen-driven immune response and a shift in the V gene repertoire compared to IgM rheumatoid factors. *Eur. J. Immunol. 23:1220.*
15. Press, J. L., and C. A. Giorgetti. 1993. Molecular and kinetic analysis of an epitope-specific shift in the B cell memory response to a multide-terminant antigen. *J. Immunol. 151:1998.*
16. Kalinke, U., E. M. Bucher, B. Ernst, A. Oxenius, H.-P. Roost, S. Geley, R. Kofler, R. M. Zinkernagel, and H. Hengartner. 1996. The role of somatic mutation in the generation of the protective humoral immune response against vesicular stomatitis virus. *Immunity 5:639.*
17. Ashton-Rickardt, P. G., and S. Tonegawa. 1994. A differential-avidity model for T-cell selection. *Immunol. Today 15:362.*
18. Arpin, C., J. Banchereau and Y.-J. Liu. 1997. Memory B cells are biased toward terminal differentiation: A strategy that may prevent repertoire freezing. *J. Exp. Med. 186:931.*
19. Perelson, A. S., and S. A. Kauffman, eds. 1991. *Molecular Evolution on Rugged Landscapes: Proteins, RNA and the Immune System*. Vol. 9 of Santa Fe Institute Studies in the Sciences of Complexity. Addison-Wesley, Redwood City, CA, p. 73.
20. Kelsoe, G. 1996. Life and death in germinal centers (redux). *Immunity 4:107.*
21. MacLennan, I., and E. Chan. 1993. The dynamic relationship between B-cell populations in adults. *Immunol. Today 14:29.*
22. Osmond, D. G. 1993. The turnover of B-cell populations. *Immunol. Today 14:34.*
23. Coutinho, A. 1993. Lymphocyte survival and V-region repertoire selection. *Immunol. Today 14:38.*
24. Rajewsky, K. 1989. Evolutionary and somatic immunological memory. In *Progress in Immunology*, Vol. 7, F. Melchers, ed. Springer-Verlag, Berlin, p. 397–403.
25. Agenes, F., M. M. Rosado, and A. A. Freitas. 1997. Independent homeostatic regulation of B cell compartments. *Eur. J. Immunol. 27:1801.*
26. Sulzer, B., L. van Hemmen, A. U. Neumann, and U. Behn. 1993. Memory in idiotypic networks due to competition between proliferation and differentiation. *Bull. Math. Biol. 55:1133.*
27. Oprea, M., and A. S. Perelson. 1996. Exploring the mechanisms of primary antibody response to T cell-dependent antigens. *J. Theor. Biol. 181:215.*
28. Kosco-Vilbois, M. H., H. Zentgraf, J. Gerdes, and J. Bonnefoy. 1997. To "B" or not to "B" a germinal center? *Immunol. Today 18:225.*
29. Shlomchik, M., P. Watts, M. Weigert, and S. Litwin. 1998. Clone: a Monte-Carlo computer simulation of B cell clonal expansion, somatic mutation, and antigen-driven selection. *Curr. Top. Microbiol. Immunol. 229:173.*
30. Oprea, M., and A. S. Perelson. 1997. Somatic mutation leads to efficient affinity maturation when centrocytes recycle back to centroblasts. *J. Immunol. 158:5155.*
31. Kepler, T. B., and A. S. Perelson. 1993. Cyclic re-entry of germinal center B cells and the efficiency of affinity maturation. *Immunol. Today 14:412.*
32. Celada, F., and P. E. Seiden. 1996. Affinity maturation and hypermutation in a simulation of the humoral immune response. *Eur. J. Immunol. 26:13508.*
33. Slifka, M. K., and R. Ahmed. 1998. Long-lived plasma cells: a mechanism for maintaining persistent antibody production. *Curr. Opin. Immunol. 10:252.*
34. Ahmed, R., and D. Gray. 1996. Immunological memory and protective immunity: understanding their relation. *Science 272:54.*